The Astrophysical Journal, 598:369–374, 2003 November 20

SMALL MAGELLANIC CLOUD–TYPE INTERSTELLAR DUST IN THE MILKY WAY

Lynne A. Valencic,[1] Geoffrey C. Clayton,[1] Karl D. Gordon,[2] and Tracy L. Smith[3]

Received 2003 June 4; accepted 2003 August 1

ABSTRACT

It is well known that the sight line toward HD 204827 in the cluster Trumpler 37 shows a UV extinction curve that does not follow the average Galactic extinction relation. However, when a dust component, foreground to the cluster, is removed, the residual extinction curve is identical to that found in the SMC within the uncertainties. The curve is very steep and has little or no 2175 Å bump. The position of HD 204827 in the sky is projected onto the edge of the Cepheus *IRAS* bubble. In addition, HD 204827 has an *IRAS* bow shock, indicating that it may be embedded in dust swept up by the supernova that created the *IRAS* bubble. Shocks due to the supernova may have led to substantial processing of this dust. The HD 204827 cloud is dense and rich in carbon molecules. The 3.4 μm feature indicating a C-H grain mantle is present in the dust toward HD 204827. The environment of the HD 204827 cloud dust may be similar to the dust associated with HD 62542, which lies on the edge of a stellar wind bubble and is also dense and rich in molecules. This sight line may be a Rosetta Stone if its environment can be related to those in the SMC having similar dust.

Subject headings: dust, extinction — Magellanic Clouds

1. INTRODUCTION

The Cardelli, Clayton, & Mathis (1989, hereafter CCM89) average Milky Way extinction relation, A_λ/A_V, is applicable to a wide range of interstellar dust environments, including lines of sight through diffuse dust and dark cloud dust, as well as dust associated with star formation. However, the CCM89 relation does not usually apply beyond the Milky Way, even in other Local Group galaxies, such as the Magellanic Clouds and M31 (e.g., Clayton & Martin 1985; Fitzpatrick 1985, 1986; Clayton et al. 1996; Bianchi et al. 1996; Gordon & Clayton 1998; Misselt, Clayton, & Gordon 1999). There is some evidence that it may apply along some sight lines in the Large Magellanic Cloud (LMC; Gordon et al. 2003). It is important to understand why dust in these other galaxies is different, since many extragalactic environments seem to contain interstellar dust that is better represented by dust in the Small Magellanic Cloud (SMC) than the Milky Way (e.g., Gordon, Calzetti, & Witt 1997; Pitman, Clayton, & Gordon 2000). Real deviations from CCM89 are seen for a few sight lines in the Galaxy (Cardelli & Clayton 1991; Mathis & Cardelli 1992). Sight lines such as those toward HD 62542, HD 204827, and HD 210121 show weak bumps and anomalously strong far-UV extinction for their measured values of R_V. Other steep far-UV, weak bump dust was found along some low-density, low-extinction sight lines (Clayton, Gordon, & Wolff 2000). The extinction along these sight lines resembles that seen in the LMC, but none approach the extreme properties of the SMC sight lines. Nevertheless, studying these anomalous Galactic sight lines may be a key to relating the differing extinction characteristics to various dust environments seen in the Milky Way and other galaxies.

The ultraviolet extinction properties of dust toward 18 stars in Trumpler 37, including HD 204827, were studied more than 15 years ago (Clayton & Fitzpatrick 1987, hereafter CF87). At that time, the UV extinction in this region of the sky was referred to as anomalous, because it was generally steeper than the average Galactic extinction curve. This extinction in the Trumpler 37 region is no longer considered anomalous. The extinction curves, with one exception, fit the CCM89 relation with R_V values less than the Galactic average of 3.1. The exception is HD 204827, which has an extinction curve significantly steeper than the appropriate CCM89 curve.

In this paper, we take advantage of improved *International Ultraviolet Explorer* (*IUE*) data along with infrared data from Two Micron All Sky Survey and *IRAS* to reinvestigate the dust associated with HD 204827 and Trumpler 37.

2. UV EXTINCTION CURVES

IUE spectra for all 18 stars in Trumpler 37, previously studied by CF87, were obtained from the Multimission Archive at Space Telescope. The archive spectra were reduced using NEWSIPS and then recalibrated using the method developed by Massa & Fitzpatrick (2000). The signal-to-noise ratio of the NEWSIPS *IUE* spectra has been improved by 10%–50% over those spectra used by CF87 (Nichols & Linsky 1996). Low-dispersion LWR/LWP and SWP spectra were selected from either aperture. Multiple spectra from one camera were averaged, and then the long and short-wavelength segments were merged at the shortest wavelength of the SWP. The wavelength coverage is ~1200–3200 Å. The sample stars and their *IUE* spectra are listed in Table 1.

The standard pair method, in which a reddened star is compared to an unreddened one of the same spectral type, was used to construct each sight line's extinction curve (Massa, Savage, & Fitzpatrick 1983). The unreddened comparison stars were selected from Cardelli, Sembach, & Mathis (1992). The spectral matches were made on the basis of comparing the UV spectra of pairs of stars rather than matching their visible spectral types. The R_V was estimated from the *JHK* colors as described in Fitzpatrick (1999); A_V was found using R_V and $E(B-V)$. The extinction curves are

[1] Department of Physics and Astronomy, Louisiana State University, Baton Rouge, LA 70803; valencic@phys.lsu.edu, gclayton@fenway.phys.lsu.edu.

[2] Steward Observatory, University of Arizona, Tucson, AZ 85721; kgordon@as.arizona.edu.

[3] Space Science Institute Columbus, Smith Laboratory, Department of Physics, Ohio State University, Columbus, OH 43210; tsmith@campbell.mps.ohio-state.edu.

TABLE 1
IUE Spectra and Photometry Sources of Program Stars

HD/BD	SWP	LWP/LWR	*UBV* Source
204827	11131, 14530	09761, 11104	1
205794	23119	03451	2
205948	23122	03453	2
206267	26011	06057, 17971	2
239683	23130	03460	2
239689	23138	03466	2
239693	23131	03463	2
239710	17470	13757	2
239722	23125	03456	3
239724	23118	03450	2
239725	23136	03464	2
239729	13451	10114	2
239738	23123	03454	3
239742	23129	03459	4
239745	23128	03458	2
239748	23137	03465	4
+57 2395B	23132	03461	3
+58 2292	23139	03467	3

Note.— All *JHK* photometry is from 2MASS.

References.—(1) Hiltner 1956. (2) Nicolet 1978. (3) Garrison & Kormendy 1976. (4) Simonson 1968.

TABLE 2
Properties of Program Stars

HD/BD	Spectral Type	UV Spectral Type	$E(B-V)$	R_V
204827	B0 V	B0 V	1.10 ± 0.05	2.58 ± 0.12
205794	B5 V	B0.5 V	0.62 ± 0.05	3.09 ± 0.26
205948	B2 V	B1 V	0.50 ± 0.04	2.90 ± 0.27
206267	O6 V	O7 V	0.52 ± 0.04	2.82 ± 0.22
239683	B5 V	B2 IV	0.54 ± 0.04	2.76 ± 0.22
239689	B5 V	B1 V	0.45 ± 0.04	2.70 ± 0.29
239693	B5 V	B4 IV	0.41 ± 0.04	2.37 ± 0.27
239710	B3 V	B1 V	0.62 ± 0.07	3.02 ± 0.32
239722	B5 V	B1 V	0.93 ± 0.05	2.86 ± 0.17
239724	B1 III	B1.5 III	0.62 ± 0.04	3.18 ± 0.24
239725	B5 V	B1 V	0.52 ± 0.04	3.14 ± 0.28
239729	B0 V	O9 V	0.66 ± 0.04	3.19 ± 0.19
239738	B5 V	B2 V	0.51 ± 0.05	2.90 ± 0.32
239742	B5 V	B4 IV	0.38 ± 0.04	2.36 ± 0.31
239745	B5 V	B1.5 V	0.54 ± 0.07	2.66 ± 0.34
239748	B5 V	B1 V	0.43 ± 0.04	2.93 ± 0.31
+57 2395B	B5 V	B2 V	0.64 ± 0.04	2.44 ± 0.19
+58 2292	B5 V	B2 V	0.57 ± 0.03	3.00 ± 0.26

normalized to A_V. Table 1 lists the sources of the *UBV* photometry. Photometry in the *JHK* bands was available for all the stars in the sample from the 2MASS database (Cutri et al. 2003). Table 2 lists the spectral type, the reddening, and the calculated R_V for each star in the sample. In general, our UV spectral classifications are in good agreement with those of CF87. The resulting extinction curves were fitted with the Fitzpatrick-Massa (FM) parameterization (Fitzpatrick & Massa 1990). The fit has been limited to the wavelength range 2700–1250 Å (3.7–8.0 μm^{-1}), because it is not reliable longward of 2700 Å (E. Fitzpatrick 2002, private communication), and the 1250 Å cutoff excludes the Lyα feature at 1215 Å. The normalization of the FM parameters was converted from $E(B-V)$ to A_V. The parameters are listed in Table 3. In Figure 1, the extinction curve and corresponding CCM89 curve for each sight line are shown.

The Cep OB2 association is a complex system with several distinct regions. Previous studies have placed it at a distance of around 800 pc (see, e.g., Garrison & Kormendy 1976; Georgelin & Georgelin 1976), although an analysis of *Hipparcos* parallaxes have placed Cep OB2 much closer, at 615 pc (de Zeeuw et al. 1999). Most of the stars in our sample are probably members of the Trumpler 37 association (Marschall & van Altena 1987; de Zeeuw et al. 1999). The possible exceptions are HD 239724, which has been placed at about 3 kpc (Simonson 1968), and HD 204827, placed at about 500 pc (CF87). However, de Zeeuw et al. (1999) give a probability of 66% that HD 204827 is a member of Cep OB2, and Marschall & van Altena (1987) give a 93%

TABLE 3
FM Parameters of Program Stars

HD/BD	c_1/R_V	c_2/R_V	c_3/R_V	c_4/R_V	x_0	γ
204827	1.08 ± 0.38	0.38 ± 0.03	0.66 ± 0.13	0.36 ± 0.06	4.66 ± 0.02	0.91 ± 0.03
205794	1.27 ± 0.40	0.17 ± 0.03	1.05 ± 0.19	0.14 ± 0.04	4.57 ± 0.01	0.88 ± 0.02
205948	1.36 ± 0.43	0.16 ± 0.03	1.17 ± 0.25	0.18 ± 0.04	4.59 ± 0.01	0.91 ± 0.03
206267	1.17 ± 0.45	0.27 ± 0.04	1.02 ± 0.20	0.22 ± 0.05	4.59 ± 0.01	0.91 ± 0.03
239683	1.21 ± 0.43	0.23 ± 0.04	1.59 ± 0.39	0.24 ± 0.07	4.59 ± 0.03	1.18 ± 0.04
239689	0.84 ± 0.27	0.28 ± 0.04	1.29 ± 0.18	0.18 ± 0.03	4.57 ± 0.005	0.96 ± 0.02
239693	1.16 ± 0.43	0.23 ± 0.05	1.13 ± 0.26	0.20 ± 0.06	4.57 ± 0.95	0.90 ± 0.03
239710	1.56 ± 0.49	0.15 ± 0.04	0.71 ± 0.18	0.20 ± 0.06	4.60 ± 0.02	0.82 ± 0.03
239722	0.88 ± 0.34	0.32 ± 0.04	1.28 ± 0.21	0.22 ± 0.04	4.59 ± 0.01	1.04 ± 0.03
239724	1.09 ± 0.35	0.21 ± 0.03	1.07 ± 0.19	0.14 ± 0.03	4.60 ± 0.01	0.94 ± 0.03
239725	1.16 ± 0.42	0.22 ± 0.03	0.87 ± 0.16	0.21 ± 0.04	4.56 ± 0.01	0.91 ± 0.03
239729	1.11 ± 0.25	0.22 ± 0.02	1.01 ± 0.16	0.25 ± 0.04	4.61 ± 0.01	1.08 ± 0.03
239738	1.00 ± 0.01	0.24 ± 0.04	1.17 ± 0.28	0.20 ± 0.06	4.55 ± 0.01	1.03 ± 0.03
239742	0.57 ± 0.33	0.38 ± 0.11	1.84 ± 0.58	0.15 ± 0.07	4.58 ± 0.02	1.03 ± 0.04
239745	1.12 ± 0.28	0.22 ± 0.04	1.36 ± 0.31	0.19 ± 0.05	4.54 ± 0.004	0.93 ± 0.02
239748	1.21 ± 0.41	0.20 ± 0.04	1.08 ± 0.25	0.25 ± 0.06	4.57 ± 0.01	0.88 ± 0.03
+57 2395B	1.28 ± 0.41	0.35 ± 0.05	1.29 ± 0.24	0.31 ± 0.06	4.57 ± 0.01	0.97 ± 0.03
+58 2292	0.94 ± 0.29	0.25 ± 0.04	1.08 ± 0.18	0.14 ± 0.03	4.58 ± 0.01	0.92 ± 0.02
204827 (partially dereddened)	-1.85 ± 0.54	0.82 ± 0.15	0.24 ± 0.09	0.11 ± 0.04	4.60 ± 0.00	1.00 ± 0.00
SMC bar average	-1.81 ± 0.16	0.83 ± 0.15	0.14 ± 0.05	0.17 ± 0.02	4.60 ± 0.00	1.00 ± 0.00

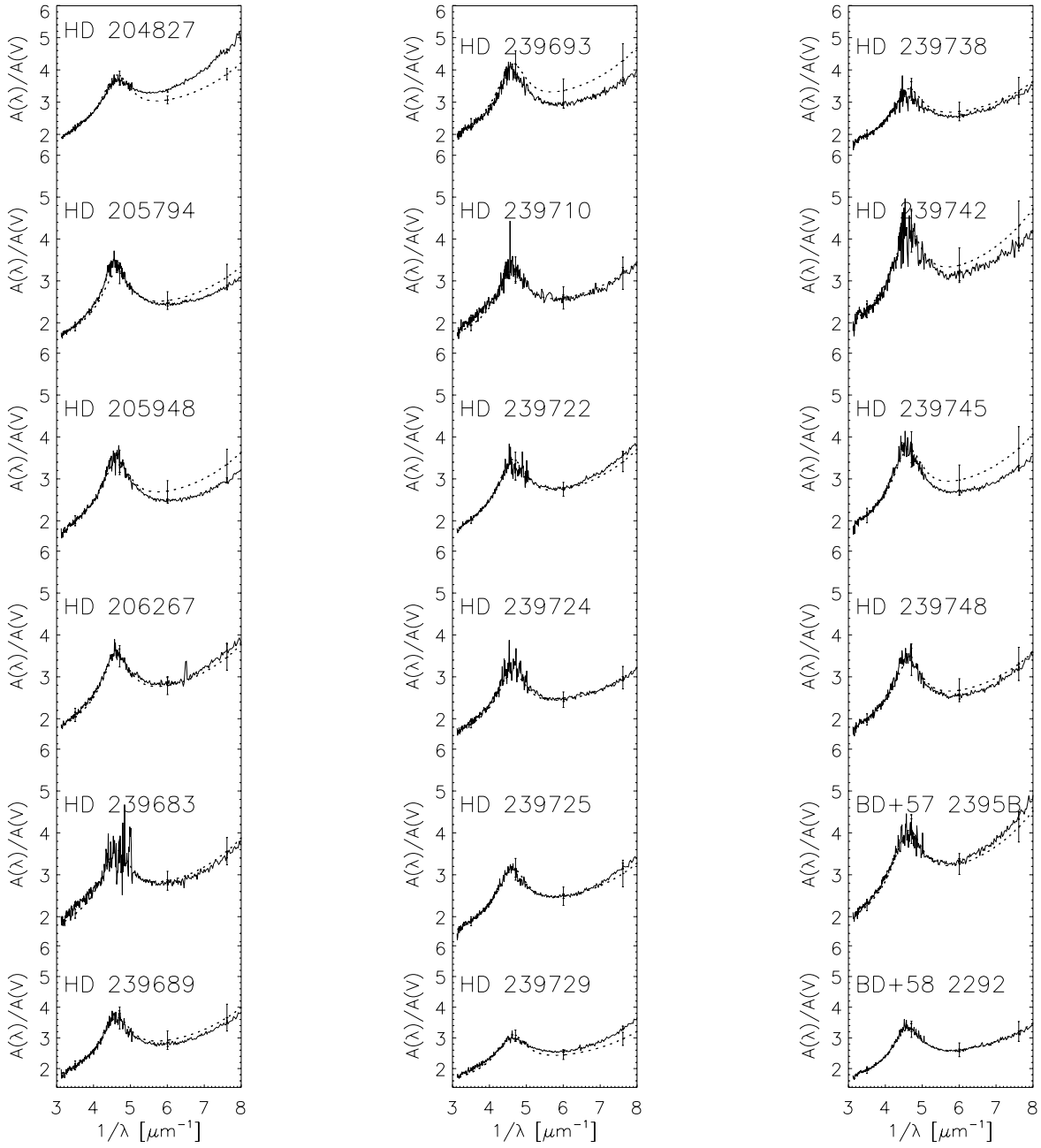

FIG. 1.—Extinction curves of the Trumpler 37 sight lines overlaid with CCM89 curves appropriate to R_V along each sight line. The error bars indicate a 1 σ uncertainty.

probability that HD 239724 is a member of Trumpler 37. The distance to HD 204827 is uncertain since it is a spectroscopic binary (Petrie & Pearce 1961; Mason et al. 1998).

With the exception of HD 204827 and HD 239722, the reddenings of all the sample stars lie between $E(B-V)$ of 0.4 and 0.6 mag. This reddening is primarily due to dust foreground to Trumpler 37. Using the average reddening per kiloparsec in the Galaxy, we would expect 0.4–0.5 mag in front of Trumpler 37 if it lies at a distance of 600–800 pc (Spitzer 1978). Therefore, only the sight lines toward HD 204827 [$E(B-V) = 1.10$] and HD 239722 [$E(B-V) = 0.93$] seem to contain significant amounts of additional dust that may be associated with Trumpler 37 itself.

The calculated values of R_V for the sample stars tend to be smaller than 3.1, although almost all the estimated R_V values are within 2 σ of 3.1. Averaging the 16 stars in the sample having low-to-moderate reddening, we get $E(B-V) = 0.53 \pm 0.01$ mag and $R_V = 2.84 \pm 0.07$. As can be seen in Figure 1, with the exception of HD 204827, none of the Trumpler 37 extinction curves deviates more than 2 σ from its corresponding CCM89 curve. The dust foreground to the Trumpler 37 appears to be normal diffuse interstellar dust adhering to the CCM89 relation.

In an effort to separate the effects of the foreground dust and dust local to the cloud, we partially dereddened the *IUE* spectra and *UBVJHK* photometry for HD 204827 and HD 239722. A CCM89-type extinction corresponding to $E(B-V) = 0.55$ mag and $R_V = 2.84$ was removed. Extinction curves were then recalculated for these two sight lines using these partially dereddened spectra, their corrected

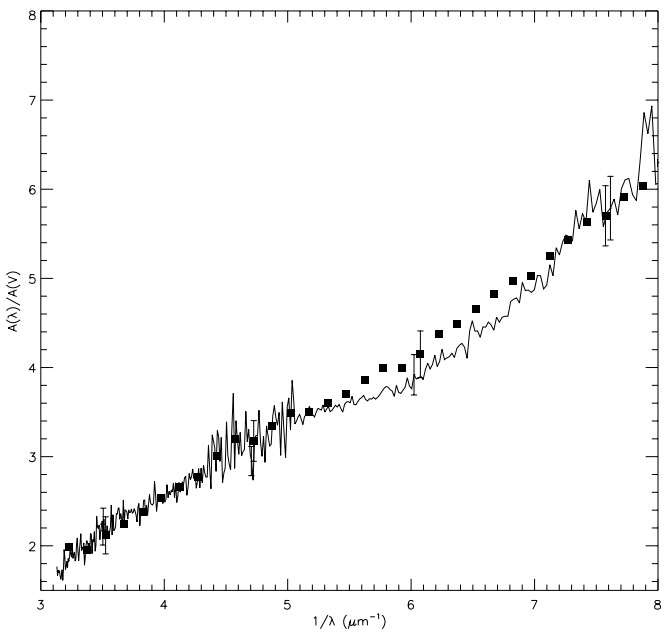

FIG. 2.—Partially dereddened extinction curve for HD 204827 (*solid line*). The extinction curve to the SMC bar (*squares*) from Gordon et al. (2003) is also shown. The error bars indicate a 1 σ uncertainty.

colors, and their original UV comparison spectra. The residual reddening toward HD 204827 from Trumpler 37 dust is $E(B-V) \sim 0.55$ mag, and toward HD 239722 it is $E(B-V) \sim 0.4$ mag. The new HD 239722 curve is not significantly different from the original curve with the foreground included. They differ by only ~ 1 σ. However, the new HD 204827 curve is significantly different (see Fig. 2). It is now extremely steep and has almost no 2175 Å bump. In fact, it is indistinguishable within the uncertainties from the average SMC bar extinction curve (Gordon et al. 2003). This has also been plotted in Figure 2. The two curves lie within 1 σ of each other.

The FM parameters for HD 204827's partially unreddened curve were also found. These are listed in Table 3, as are the average values for the SMC bar (Gordon et al. 2003). They were found with the same method that Gordon et al. (2003) used to find FM parameters for the SMC Bar sight lines. This required holding x_0 and γ fixed at 4.60 and 1.00, respectively, while varying the other parameters such that χ^2 was minimized. Again, these values are within each other's uncertainties.

2.1. *IR Emission*

Figure 3 shows $0.^\circ5 \times 0.^\circ5$ *IRAS* HiRes images centered on HD 204827 in the 25 and 60 μm bands (Aumann, Fowler, & Melnyk 1990). *IRAS* HiRes images have spatial resolution better than 1′ and fluxes good to 20%. HD 204827 shows an apparent bow shock in the 25 and 60 μm images (van Buren & McCray 1988). Integrated fluxes in Janskys were found over a square aperture of 25′ on each side. The background flux was also found and removed. The measured fluxes are listed in Table 4, along with the color temperatures estimated from the flux ratios (Ward-Thompson & Robson 1991). These are similar to T_d in bow shocks found elsewhere (Ward-Thompson & Robson 1991; van Buren & McCray 1988). We also fitted the *IRAS* fluxes with a blackbody curve. A temperature of $\sim$75 K yielded the best fit for the data.

Bow shocks are generally associated with early-type runaway stars having peculiar space velocities in excess of 30 km s^{-1} (Blauuw 1961). Using the observed radial velocity of HD 204827 (Gies 1987) and its *Hipparcos* proper motions, we calculate the peculiar space velocity $v_{\rm space}^{\rm pec} = 35.1 \pm 25.2$ km s^{-1}. Since the uncertainty in the velocity is rather large, we can only say that the velocity HD 204827 is consistent with being a runaway star. The standoff distance of the HD 204827 bow shock (4.′5, or 0.9 pc at a distance of 650 pc) seen in Figure 3 is also consistent with this velocity and the standard assumptions made in Van Buren & McCray (1988).

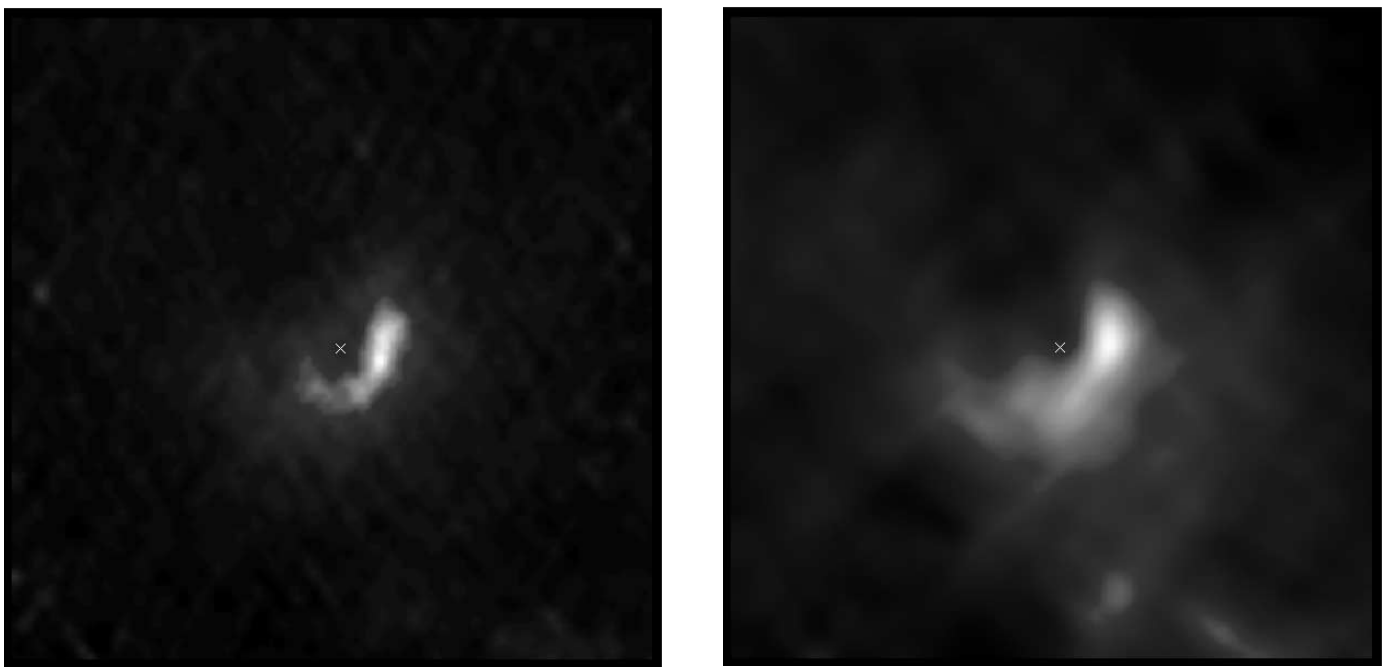

FIG. 3.—$0.^\circ5 \times 0.^\circ5$ *IRAS* HiRes images of HD 204827 at 25 (*left*) and 60 μm (*right*). The cross indicates the star's location.

TABLE 4
IRAS FLUXES AND COLOR TEMPERATURES FOR HD 204827

Parameter	Value
$F(12\ \mu m)$ (Jy)	0.14 ± 0.08
$F(25\ \mu m)$ (Jy)	27.84 ± 1.11
$F(60\ \mu m)$ (Jy)	170.27 ± 4.43
$F(100\ \mu m)$ (Jy)	146.03 ± 14.84
$T_{12/25}$ (K)	70 ± 7
$T_{25/60}$ (K)	55 ± 1
$T_{60/100}$ (K)	38 ± 3

2.2. *IR Spectroscopy*

In 2001 and 2002 August, IR spectra of HD 204827 and HD 239722 (the other highly reddened cluster member) were obtained with the SpeX instrument at the NASA Infrared Telescope Facility (IRTF). SpeX is a medium-resolution spectrograph that can cover a wavelength range from 0.8 to 5.5 μm. For this investigation, the 1.9–4.2 μm, cross-dispersed mode was used. These data were reduced using version 2.0 of the associated SPEXTOOL software (Cushing, Vacca, & Rayner 2003; Rayner et al. 2003). To remove telluric lines, the spectrum of a ratioing G star was obtained at the same time, with observations bracketing those of the program star. The difference in air mass between the target and the G star averaged 0.02, and they were separated by less than 1° on the sky. The reduced target spectrum was then multiplied by a solar spectrum scaled to match the G star so that the stellar lines introduced by the division would be removed. The resulting spectrum then had a blackbody curve removed, corresponding to the effective temperature of the UV spectral classification. Optical depth plots were then derived, following the method of Sandford et al. (1991), by fitting and removing a linear baseline to the reduced spectrum between 3.23 and 3.64 μm. For HD 204827, the feature's optical depth was then measured at 3.42 μm (Pendleton et al. 1994), yielding $\tau_{3.4} = 0.0139 \pm 0.0036$.

HD 204827's optical depth plot is shown in Figure 4 (*top*), overlaid with the spectrum of the Murchison meteorite (de Vries et al. 1993) and a zero line for easier comparison. The 3.4 μm aliphatic C—H stretch is weak, but present. The middle panel of Figure 4 shows the optical plot with the scaled Murchison spectrum subtracted for emphasis. This feature arises from an organic carrier in the diffuse interstellar medium (ISM). Pendleton et al. (1994) used a sample of sight lines, with $A_V \geq 3.9$ mag, to show that there is a correlation between A_V and the feature's optical depth $\tau_{3.4}$, with the average value of $A_V/\tau_{3.4} = 270 \pm 40$ in the diffuse ISM. Our value of $A_V/\tau_{3.4} = 205 \pm 63$ is in agreement with their results. Thus, the sight line toward HD 204827 sets a new lower limit on the extinction ($A_V = 2.84 \pm 0.13$) at which the feature has been detected. There is no detectable 3.1 μm water ice feature (Pendleton et al. 1994 and references therein). HD 239722 does not show a significant 3.4 μm feature, with $\tau_{3.4} = 0.010 \pm 0.006$, although this sight line has a similar amount of extinction ($A_V = 2.66 \pm 0.18$ mag) to HD 204827. Accordingly, HD 239722's $A_V/\tau_{3.4}$ ($=266 \pm 178$) is not significant. Its spectrum is shown in Figure 4 (*bottom*), again with a zero line for contrast.

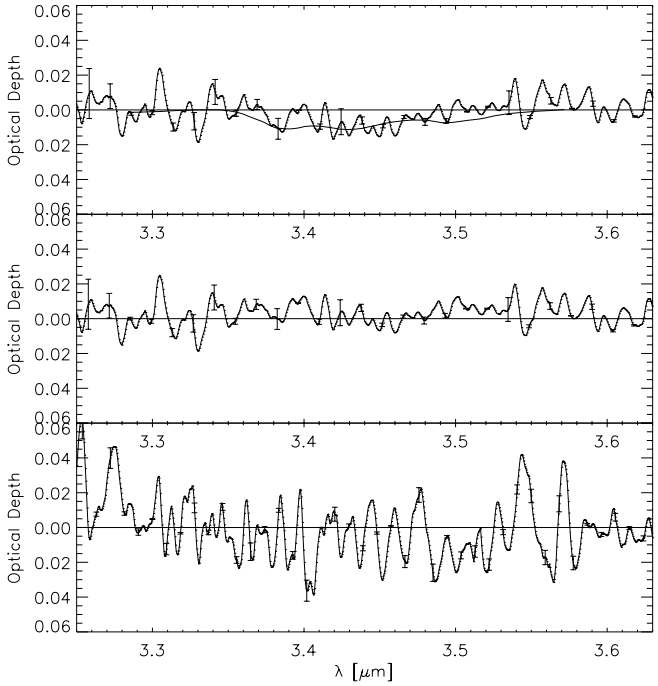

FIG. 4.—Optical depth plots of HD 204827 and HD 239722 for comparison. Both were obtained with SpeX. *Top*: HD 204827 with the C-H aliphatic stretch at 3.4 μm overlaid (de Vries et al. 1993). *Middle*: HD 204827 with the 3.4 μm feature removed for emphasis. *Bottom*: HD 239722; no feature is visible. The error bars represent 1 σ uncertainty.

3. DISCUSSION

The residual sight line toward HD 204827 with the foreground dust component removed is unique in the Galaxy. About 400 hundred sight lines in the Galaxy have measured UV extinction curves, and no other sight line in the Galaxy shows an extinction curve resembling that seen in the SMC bar (Gordon & Clayton 1998; L. Valencic 2003, in preparation). This includes the sight lines nearby HD 204827 in the sky, which are seen in Figure 1. So the HD 204827 sight line is sampling dust not seen along the nearby sight lines toward Trumpler 37 and Cep OB2. For the purposes of this discussion, we shall refer to this dust as HD 204827 cloud dust. Using a similar method, Whittet et al. (2003) find a bumpless residual dust component but with a flatter UV extinction toward HD 283809 in the Taurus Cloud.

HD 204827 lies in the outer part of the Trumpler 37 cluster, away from any bright rims or areas of nebulosity, north-northwest of IC 1396. Its projected position also lies right on the edge of the Cepheus *IRAS* bubble (Patel et al. 1998). The *IRAS* 100 μm image reveals that the position of HD 204827 is projected on the edge of a peninsula of higher optical depth (Abraham, Balazs, & Kun 2000). The presence of the bow shock around HD 204827 indicates that the star may lie in or near the material swept up in the formation of the bubble. It formed through a combination of stellar winds and a supernova explosion from the first generation of star formation in the region, NGC 7160, which occurred about 7 Myr ago (Patel et al. 1998). The Trumpler 37 cluster formed about 5 Myr ago perhaps induced by the formation of the Cepheus bubble. Shocks such as those in supernova ejecta will produce a dust grain size distribution skewed toward smaller grains. This will lead to a steeper far-UV

extinction but should also lead to a stronger 2175 Å bump, since this feature is also believed to result from a population of small grains. (O'Donnell & Mathis 1997).

The four sight lines in the SMC that show extinction similar to that seen toward the HD 204827 dust cloud have quite small reddenings [$E(B-V) \sim 0.2$ mag]. In addition, they are low-density diffuse ISM sight lines where the dust could have easily been subjected to processing by UV radiation and shocks (Gordon & Clayton 1998; Gordon et al. 2003). A group of similar sight lines in the Galaxy sampling very low density ISM showed weak bumps and steep non-CCM89 far-UV extinction (Clayton et al. 2000). But the weakness of the bumps and the steepness of the far-UV extinction of these sight lines do not approach that seen in the SMC. These Galactic sight lines are more similar to those associated with an LMC2 superbubble (Misselt et al. 1999; Gordon et al. 2003).

The environment of the dust in the HD 204827 cloud is quite different from that seen in the SMC sight lines. The column density of the dust [$E(B-V) = 0.55$ mag] in the HD 204827 dust cloud is larger, but the cloud also has a much higher density. The HD 204827 dust cloud resembles a molecular cloud more than the diffuse ISM. The cloud is very rich in carbon molecules, showing large column densities of C_2, C_3, CH, and CN (Oka et al. 2003; Thorburn et al. 2003). In this respect, the HD 204827 cloud dust is quite similar to the sight line toward HD 62542 (Cardelli & Savage 1988). This sight line shows a severely non-CCM89 sight line with a broad bump and steep far-UV extinction. Its dust is also rich in carbon molecules. The projected position of HD 62542 lies on the edge of material swept up by a stellar wind bubble. Three other non-CCM89, weak-bump, steep far-UV sight lines in the Galaxy, HD 283809, HD 29647, and HD 210121, are also associated with dense clouds (Cardelli & Savage 1988; Larson, Whittet, & Hough 1996; Cardelli & Wallerstein 1989; Gordon et al. 2003). The dust in the molecular cloud associated with HD 210121 is likely to have been processed as it was propelled into the halo during a Galactic fountain or other event. The other two sight lines toward HD 29647 and HD 283809 seem to be sampling dust in quiescent dense clouds. These two sight lines show a strong 3.1 μm ice feature and a weak 3.4 μm feature similar to the one seen in the HD 204827 cloud dust (Goebel 1983; Smith, Sellgren, & Brooke 1993). The steep far-UV extinction in these clouds helps shield the molecules in these clouds from dissociating UV radiation leading to larger column densities than might be found in clouds with less steep far-UV extinction (Mathis 1990).

So the conditions for producing SMC-type extinction exist in our own Galaxy. Those conditions are not necessarily associated with low-reddening, low-density, diffuse ISM environments. Also, metallicity differences between the Galaxy and the SMC may not be a determining factor. This supports results that find SMC-type extinction in starburst galaxies having a wide range of metallicities (Calzetti, Kinney, & Storchi-Bergmann 1994; Gordon et al. 1997).

Financial support was provided by the Louisiana Board of Regents, BoRSF, under agreement NASA/LEQSF (1996–2001)–LaSPACE-01 or NASA/LEQSF (2001–2005)–LaSPACE and NASA/LaSPACE under grant NGC 5-40115.

REFERENCES

Abraham, P., Balazs, L. G., & Kun, M. 2000, A&A, 354, 645
Aumann, H. H., Fowler, J. W., & Melnyk, M. 1990, AJ, 99, 1674
Bianchi, L., Clayton, G. C., Bohlin, R. C., Hutchings, J. B., & Massey, P. 1996, ApJ, 471, 203
Blaauw, A. 1961, Bull. Astron. Inst. Netherlands, 15, 265
Calzetti, D., Kinney, A. L., & Storchi-Bergmann, T. 1994, ApJ, 429, 582
Cardelli, J., & Clayton, G. 1991, AJ, 101, 1021
Cardelli, J., Clayton, G., & Mathis, J. 1989, ApJ, 345, 245 (CCM89)
Cardelli, J., & Savage, B. 1988, ApJ, 325, 864
Cardelli, J., Sembach, K. R., & Mathis, J. S. 1992, AJ, 104, 1916
Cardelli, J., & Wallerstein, G. 1989, AJ, 97, 1099
Clayton, G. C., & Fitzpatrick, E. L. 1987, AJ, 93, 157 (CF87)
Clayton, G. C., Gordon, K. D., & Wolff, M. J. 2000, ApJS, 129, 147
Clayton, G. C., Green, J., Wolff, M., Zellner, N., Code, A., Davidsen, A., WUPPE Science Team, and HUT Science Team. 1996, ApJ, 460, 313
Clayton, G. C., & Martin, P. G. 1985, ApJ, 288, 558
Cutri, R. M., et al. 2003, 2MASS Second Incremental All Sky Point Source Catalog
De Vries, M. S., Reihs, K., Wendt, H. R., Golden, W., Hunziker, H., Flemming, R., Peterson, E., & Chang, S. 1993, Geochim. Cosmochim. Acta, 57, 933
De Zeeuw, P. T., Hoogerwerf, R., de Bruijne, J. H. J., Brown, A. G. A., & Blaauw, A. 1999, AJ, 117, 354
Fitzpatrick, E. L. 1985, ApJS, 59, 77
———. 1986, AJ, 92, 1068
———. 1999, PASP, 111, 63
Fitzpatrick, E., & Massa, D. 1990, ApJS, 72, 163
Garrison, R. F., & Kormendy, J. 1976, PASP, 88, 865
Georgelin, Y. M., & Georgelin, Y. P. 1976, A&A, 49, 57
Gies, D. R. 1987, ApJS, 64, 545
Goebel, J. H. 1983, ApJ, 268, L41
Gordon, K., Calzetti, D., & Witt, A. 1997, ApJ, 487, 625
Gordon, K., & Clayton, G. 1998, ApJ, 500, 816
Gordon, K., Clayton, G., Misselt, K., Landolt, A., & Wolff, M. 2003, ApJ, 594, 279
Hiltner, W. A. 1956, ApJS, 2, 389
Larson, K. A., Whittet, D. C. B., & Hough, J. H. 1996, ApJ, 472, 755
Marschall, L. A., & van Altena, W. F. 1987, AJ, 94, 71
Mason, B. D., Gies, D. R., Hartkopf, W. I., Bagnuolo, W. G., Jr., Brummelaar, T. T., & McAlister, H. A. 1998, AJ, 115, 821
Massa, D., & Fitzpatrick, E. L. 2000, ApJS, 126, 517
Massa, D., Savage, B. D., & Fitzpatrick, E. L. 1983, ApJ, 266, 662
Mathis, J. 1990, ARA&A, 28, 37
Mathis, J., & Cardelli, J. 1992, ApJ, 398, 610
Misselt, K., Clayton, G., & Gordon, K. 1999, ApJ, 515, 128
Nichols, J. S., & Linsky, J. L. 1996, AJ, 111, 517
Nicolet, B. 1978, A&AS, 34, 1 1996, AJ, 111, 517
O'Donnell, J. E., & Mathis, J. S. 1997, ApJ, 479, 806
Oka, T., Thorburn, J. A., McCall, B. J., Friedman, S. D., Hobbs, L. M., Sonnentrucker, P., Welty, D. E., & York, D. G. 2003, ApJ, 582, 823
Patel, N. A., Goldsmith, P. F., Heyer, M. H., Snell, R. L., & Pratap, P. 1998, ApJ, 507, 241
Pendleton, Y. J., Sandford, S. A., Allamandola, L. J., Tielens, A. G. G. M., & Sellgren, K. 1994, ApJ, 437, 683
Petrie, R. M., & Pearce, J. A. 1961, Publ. Dom. Astrophys. Obs. Victoria, 12, 1
Pitman, K. M., Clayton, G. C., & Gordon, K. D. 2000, PASP, 112, 537
Rayner, J. T., Toomey, D. W., Onaka, P. M., Denault, A. J., Stahlberger, W. D., Vacca, M. C., Cushing, M. C., & Wang, S. 2003, PASP, 115, 362
Sandford, S. A., Allamandola, L. J., Tielens, A. G. G. M., Sellgren, K., Tapia, M., & Pendleton, Y. 1991, ApJ, 371, 607
Simonson, S. C. 1968, ApJ, 154, 923
Smith, R. G., Sellgren, K., & Brooke, T. Y. 1993, MNRAS, 263, 749
Spitzer, L. 1978, Physical Processes in the Interstellar Medium (New York: Wiley)
Thorburn, J. A., et al. 2003, ApJ, 584, 339
Vacca, W. D., Cushing, M. C., & Rayner, J. T. 2003, PASP, 115, 389
Van Buren, D., & McCray, R. 1988, ApJ, 329, L93
Ward-Thompson, D., & Robson, E. I. 1991, MNRAS, 248, 670
Whittet, D., Senoy, S., Clayton, G., & Gordon, K. 2003, in ASP Conf. Ser., Astrophyics of Dust, ed. A Witt & G. Clayton (San Francisco: ASP), in press